Journal of Applied Physics

PLEASE CITE THIS ARTICLE AS DOI: 10.1063/5.0018909

Atomistic investigation of the temperature and size dependence of the energy barrier of CoFeB/MgO nanodots

A. Meo,[1, a)] R .Chepulskyy,[2] D .Apalkov,[2] R. W. Chantrell,[1] and R. F. L. Evans[1]
[1)]*Department of Physics, University of York, Heslington, York YO10 5DD United Kingdom.*
[2)]*Samsung Electronics, Semiconductor R&D Center (Grandis), San Jose, CA 95134, USA*

The balance between low power consumption and high efficiency in memory devices is a major limiting factor in the development of new technologies. Magnetic random access memories (MRAM) based on CoFeB/MgO magnetic tunnel junctions (MTJs) have been proposed as candidates to replace the current technology due to their non-volatility, high thermal stability and efficient operational performance. Understanding the size and temperature dependence of the energy barrier and the nature of the transition mechanism across the barrier between stable configurations is a key issue in the development of MRAM. Here we use an atomistic spin model to study the energy barrier to reversal in CoFeB/MgO nanodots to determine the effects of size, temperature and external field. We find that for practical device sizes in the 10-50 nm range the energy barrier has a complex behaviour characteristic of a transition from a coherent to domain wall driven reversal process. Such a transition region is not accessible to simple analytical estimates of the energy barrier preventing a unique theoretical calculation of the thermal stability. The atomistic simulations of the energy barrier give good agreement with experimental measurements for similar systems which are at the state of the art and can provide guidance to experiments identifying suitable materials and MTJ stacks with the desired thermal stability.

I. INTRODUCTION

The balance between low power consumption and high speed in memory devices is one of the most limiting factors in the development of new energy efficient memory technologies. Magnetic random access memory (MRAM), a storage technology where the data is stored as magnetic states rather than electrical charge, has been proposed as a candidate able to address the power issue because of its non-volatility, while maintaining high performance in writing and reading processes. The main component of a MRAM is the magnetic tunnel junction (MTJ), a multilayer structure composed, in its simplest design, of two metallic ferromagnets sandwiching a thin non-magnetic insulator. CoFeB/MgO-based MTJs exhibit high thermal stability, low threshold current and high tunnelling magneto-resistance (TMR) signal and thus they are among the most promising candidates for commercial MRAM. Nevertheless, such technology needs to maintain these features when scaled below 40 nm in the lateral dimension in order to compete with the density of current silicon-based devices.

MRAMs are bi-stable devices characterised by uniaxial anisotropy and the difference in energy between the stable (magnetisation aligned along the easy axis) and unstable (magnetisation aligned perpendicular the easy axis) states provides the energy barrier (E_b) between the two energy minima of the system against unwanted transitions caused by the thermal excitation. Understanding the size and temperature dependence of E_b and the nature of the transition mechanism across the barrier between stable configurations is a key challenge in the development of MRAM. Experimental studies have investigated the energy barrier of magnetic tunnel junctions (MTJs) as function of size[1–6]. Gajek *et al.*[6] determine the energy barrier via measurements of the switching current as a function of the switching frequency and find that the energy barrier scales quadratically with the diameter of the device as expected for a macrospin. A sharp change in the size dependence of the energy barrier resembling a linear trend for diameters larger than 30 nm can be observed in Fig. 3 of the same work and the average coercivity of the whole MTJ junction flattens for larger dimensions. Sato *et al.*[1,2,3], Sun *et al.*[4], Takeuchi *et al.*[5] found values lower than expected from a macrospin model for a system larger than the estimated single domain size, which suggests domain nucleation as the reversal mechanism. In a recent work Enobio *et al.*[7] extract the energy barrier for MTJs similar to those investigated by[5] via retention time measurements. They conclude that the crossing over the energy barrier might be described by a magnetic reversal mechanism different from nucleation. According to their reasoning the energy barrier is independent of the junction diameter in case of nucleation and the fact that they find a dependence on the MTJ diameter calls for some different explanation. The theoretical analysis performed so far on similar systems[8–10] are based on zero temperature micromagnetic modelling. The continuum approach on which standard micromagnetism is developed begins to fail with the miniaturisation of devices down to a few nanometres due to the inability to describe elevated temperatures, surface and interfacial effects and complex magnetic ordering[11]. Furthermore, the effect of temperature has been experimentally investigated only by Takeuchi *et al.*[5].

Here we study the energy barrier to magnetisation reversal in CoFeB/MgO nanodots focusing on its size, temperature and field dependence using an atomistic spin model. The results show a dependence of the energy barrier for a given thickness and temperature which scales quadratically with the diameter for systems smaller than the estimated single domain size, whereas the trend becomes linear for larger dimensions. The former behaviour can be explained by a macrospin and the coherent reversal mechanism, while the latter is characteristic of

[a)]Electronic mail: andrea.m@msu.ac.th, now working at Mahasarakham University (Thailand)

a domain wall mediated switching process.

II. METHODS

The magnetic anisotropy in CoFeB/MgO layers arises from hybridisation of Fe and O atomic orbitals at the interface[12,13]. The result is a dominant 2-ion anisotropy and complex interface magnetic ordering which can give rise to non-monotonic temperature dependence of the anisotropy[11]. This suggests that an atomistic model is appropriate for basic investigations of CoFe/MgO layers. The full complexity of this behavior, however, requires the full (long-ranged) tensor form of exchange, which makes the calculations computationally expensive. Here we use a nearest-neighbour exchange and concentrate on investigating the size dependence of the energy barrier including the effect of the applied and demagnetizing fields. However, the localized nature of the magnetic anisotropy requires atomistic simulations.

We perform simulations based on the atomistic spin model as implemented in the VAMPIRE software package[14] with a localised Heisenberg approximation for the exchange:

$$\mathcal{H} = -\sum_{i<j} J_{ij}\vec{S}_i\cdot\vec{S}_j - \sum_i k_{\rm u}^i(\vec{S}_i\cdot\hat{e})^2 - \sum_i \mu_{\rm s}^i\vec{S}_i\cdot\vec{\rm B}_{\rm app} + \mathcal{H}_{\rm dmg}. \tag{1}$$

J_{ij} is the exchange coupling constant for the interaction between the spins on site i and j, $k_{\rm u}^i$ is the uniaxial energy constant on site i along the easy-axis $\hat{e}$, $\mu_{\rm s}^i$ is the atomic spin moment on the atomic site i and $\vec{\rm H}_{\rm app}$ is the external applied field. The magnetostatic contributions $\mathcal{H}_{\rm dmg}$ to the energy of the system are calculated using a modified macrocell approach where the contribution within each cell is taken into account following the approach proposed by Bowden[15], explicitly computing the interaction tensor from the atomistic coordinates. To obtain the energy barrier and its temperature dependence we use the constrained Monte Carlo (cMC) algorithm, a modified Monte Carlo (MC) algorithm[16] with an adaptive spin update algorithm[17]. A standard MC algorithm allows the determination of the magnetic properties at thermal equilibrium. In such a condition we cannot access the magnetic anisotropy since the magnetisation aligns along the equilibrium direction, generally the easy-axis. To circumvent this, one can keep the system in a quasi equilibrium state. Such an approach has been exploited in the cMC method, which acts on two spins simultaneously and allows the direction of the global magnetisation to be constrained during the simulation along specific directions, whilst allowing individual spins $\vec{S}_i$ to reach thermal equilibrium. Since the system is not in equilibrium, the total internal torque $\vec{\tau}$ acting on the magnetisation $\vec{M}$[16] does not vanish. For a system at constant temperature the magnitude of the torque acting on the system, whose magnitude represents the work done on the system, can be expressed as:

$$\vec{\tau} = -\frac{\partial\mathcal{F}}{\partial\vartheta}, \tag{2}$$

where ϑ is the constraining direction and $\mathcal{F}(\vec{\rm M})$ is the Helmholtz free energy of the system which measures the amount of work that can be obtained in a physical system at constant temperature and volume. We can then compute the anisotropy energy as the variation of the free energy:

$$\Delta\mathcal{F} = -\int d\vartheta\vec{\tau}. \tag{3}$$

Calculating $\Delta\mathcal{F}$ at different temperatures allows the reconstruction of the temperature dependence of the effective magnetic anisotropy. Both MC approaches provide a natural way to include temperature effects. In these MC algorithms each step is at constant temperature and the temperature determine the acceptance probability expression where the internal energy of the system is compared with the thermal energy of the thermostat[16]. This differ from magnetisation or spin dynamics where a thermal field is included to account for thermal effects.

We model CoFeB/MgO nanodots, the constituent of a MTJ, as cylindrical alloy films with a body-centred cubic (BCC) crystal structure with lattice constant 2.86 Å. We model CoFeB/MgO interface with a large perpendicular uniaxial single-ion anisotropy and the value is derived from experimental measurements of the temperature dependence of the anisotropy energy density $K_{\rm u}$ of CoFeB/MgO thin films by Sato *et al.* [18]. The bottom interfacial atomic layer of CoFeB is assumed to have no particular interfacial properties and we neglect the bulk anisotropy of CoFeB, which is known to be small[19]. By exploiting the relatively small difference between on-site and two-sites anisotropy components at the temperatures of interest in this work and the lighter computational effort required by single-ion anisotropy, we treat the interfacial anisotropy as single-site. Two-ion anisotropy contributions to the anisotropy together with Dzyaloshinskii-Moriya interactions will be object of further more complex studies. The atomistic exchange parameters, J_{ij}, are extracted from a mean field approximation:

$$J_{ij} = \frac{3k_{\rm B}T_{\rm c}}{\varepsilon z}, \tag{4}$$

where $k_{\rm B}$ is the Boltzmann constant, z the number of nearest neighbours, ε is a correction due to spin waves excitations[20,21] and $T_{\rm c}$ is the Curie temperature. The interface ($z = 4$) and bulk ($z = 8$) values are determined by imposing that they exhibit the same $T_{\rm c}$, whose value we obtain from CoFeB/MgO thin films measurements performed by Sato *et al.* [18]. We describe CoFeB with an atomic spin moment $\mu_{\rm s}$ of 1.6 $\mu_{\rm B}$, corresponding to $M_{\rm s}$ about 1.3 MA m^{-1}. This value is close to the experimental reports on similar systems and yield a perpendicular anisotropy as in experiments[19], as discussed in more detail in reference[22]. Following both experimental[19,23] and theoretical[24] works that report an increase of the Gilbert damping when the thickness of the CoFeB film is reduced, we characterise the interface CoFeB/MgO with a large damping, 0.11, whereas the rest of the CoFeB has low damping. However, we point out that the damping is not accounted for when performing simulations with Monte Carlo approaches as we evaluate energies. A list of the parameters used in our simulations is reported in Table II.

TABLE I. Simulation parameters for the investigated systems.

	CoFeB(@interface)	CoFeB(bulk)	Unit
J_{ij}	1.547×10^{-20}	7.735×10^{-21}	J link^{-1}
μ_s	1.6	1.6	μ_B
k_u	1.35×10^{-22}	0.0	J atom^{-1}
α	0.11	0.003	

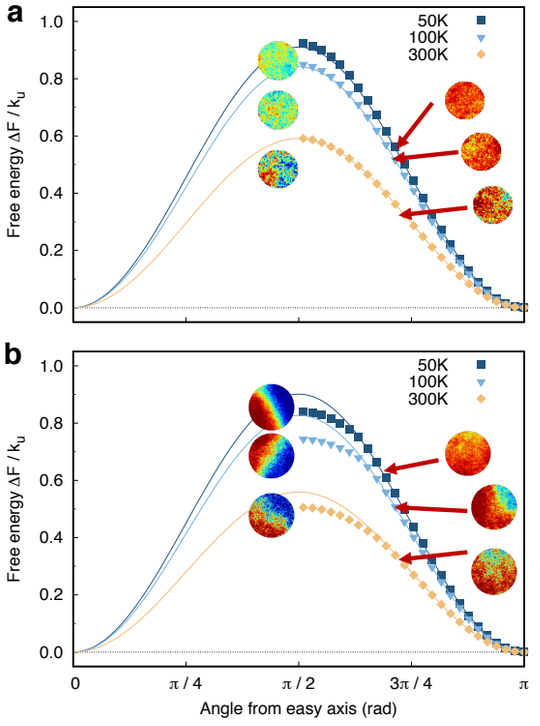

FIG. 1. Angular dependence of scaled the energy barrier scaled by the uniaxial energy constant at 0 K for a 10 nm (a) and 30 nm (b) dot. The insets show snapshots of the out-of-plane component of the magnetisation (red = spin-down, green = in-plane, blue = spin-up) at 50 K, 100 K and 300 K for constraint angles of the magnetisation of $\pi/2$ and $2/3\pi$. Lines are the fit of the data in the region $[4/5\pi : \pi]$ with a $\sin(\vartheta)^2$ function.

III. RESULTS

Here we focus on the size and temperature dependence of the energy barrier and the mechanism of the transition over the barrier in CoFeB/MgO nanodots of thickness 1 nm. Moreover, we have determined the role of an external magnetic field on the energy barrier and investigated the reversal mechanism.

A. Thermal stability in zero field

We use the cMC algorithm, described in the methods section, to calculate the angular dependence of the restoring torque via the constraint of the total magnetisation away from the easy-axis direction at different temperatures and diameters. Using the cMC method we compute the total torque acting on the magnetisation and by integrating this over the angular distribution we obtain the effective energy barrier separating the two stable states of the system. Fig. 1 presents the angular dependence of the free energy for diameters 10 nm and 30 nm at different temperatures. The 10 nm dot closely follows the $\sin(\vartheta)^2$ behaviour characteristic of a uniaxial system and coherent reversal, where ϑ is the angle formed by magnetisation and easy axis. Snapshots of the out-of-plane spin configuration, shown in the inset of Fig. 1(a), confirm the coherent nature of the reversal, even though thermal effects cause large fluctuations at small system dimensions and the switching is not completely coherent. The free energy of the 30 nm disc deviates from the above trend decreasing as angles approach $\pi/2$. This is consistent with a nucleation-type reversal and results in a lower energy barrier than for a coherent mechanism, which is often assumed in MTJ devices, and is confirmed by the spin configurations in Fig. 1(b). This decrease of the energy barrier in case of nucleation poses issues for technological applications as it yields a lower thermal stability than predicted using a macrospin model and also induces an intrinsic stochastic character to the reversal as the wall velocity during reversal can be reduced due to pinning sites.

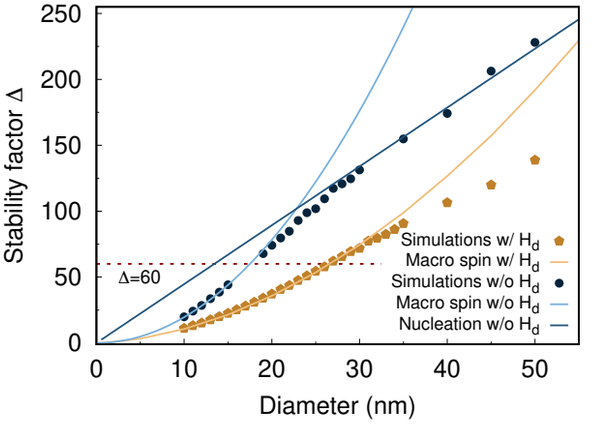

FIG. 2. Stability factor (Energy barrier/k_BT) as function of diameter for CoFeB/MgO dots at 300 K. Black dots and blue lines represent data and fit for simulations without magnetostatic interactions, orange diamonds and yellow line describe data and fit for simulations with magnetostatic interactions.

One of the most relevant parameters for applications is the stability factor Δ, defined as the energy barrier normalised by the thermal energy k_BT, where k_B is Boltzmann constant and T the absolute temperature. For technological applications such as storage devices, a stability factor larger than 60 at room temperature is required in order to guarantee a data retention of at least ten years. In Fig. 2 (yellow line and orange diamonds) we show the size dependence at room temperature of Δ. Δ is quadratic for dots smaller than 20 nm, whereas it starts deviating towards a linear trend for larger sizes. The existence of different regimes can be understood in terms of the reversal mechanism of the magnetisation: if the reversal is

coherent, E_b follows the macrospin behaviour and is given by the analytic expression $E_b = K_{eff}V$[25], where K_{eff} is the effective magnetocrystalline energy density and $V = \pi t d^2/4$ is the disc volume. In case of nucleation E_b can be obtained from the energy of a domain wall in the centre of the disc $E_b = \sigma w$, where $\sigma = 4\sqrt{A_s/K_{eff}}$ is the domain wall surface energy density, A_s the exchange stiffness and $w = dt$ is the surface of the disc of the disc[25]. The former yields a quadratic scaling of E_b with the diameter, whereas the latter linear, in agreement with the trend of the data. The single domain limit gives a criterion to predict in which of the two regimes the system falls: macrospin if the diameter is larger than the domain wall width $\delta_{DW} = \pi\sqrt{A_s/K_{eff}}$, nucleation otherwise. K_{eff} includes both the magnetocrystalline anisotropy K_u and the shape contribution arising from the long-range dipole-dipole interaction among the spins. For a uniformly magnetised cylinder the magnetostatic contribution can be written in terms of the demagnetisation tensor N:

$$K_{eff} = K_u - \frac{1}{2}\mu_0 M_s^2 \frac{(N_{zz}-1)}{2}. \quad (5)$$

Here M_s is the saturation magnetisation and N_{zz} is the zz component of the demagnetisation tensor. The second term on the RHS of equation (5) is the demagnetising energy for a cylinder which is magnetised along the easy axis direction z and $(N_{zz}-1)$ comes from $(N_{xx}+N_{yy}+N_{zz}) = 1$ in *SI* units. As the demagnetisation energy favours magnetisation alignment along the largest dimension, this contribution yields a smaller anisotropy energy for thin cylinders causing a broadening of the domain wall width and a reduction in the energy barrier, compared with a case where this term is neglected. The same expression should not be used for non-uniform magnetisation configurations since the demagnetisation tensor is a macroscopic quantity defined for a uniformly magnetised system. If we consider a system with an infinitesimal wall in the centre of the system separating two magnetic domains of equal volume, its magnetostatic contribution should be zero. However, we cannot properly compute the magnetostatic energy of this magnetic configuration using equation (5). Since an analytic formulation for non-uniform magnetised systems is not easily accessible, we compute the size and temperature dependence of E_b neglecting the magnetostatic interaction as well, so that $K_{eff} = K_u$.

We compare our data obtained with and without the inclusion of magnetostatic interactions with the analytic expression for a macrospin system, where we derive the parameters A_s ($\sim 20\times10^{-12}\,\mathrm{Jm^{-1}}$) and K_u ($\sim 1\times10^{6}\,\mathrm{Jm^{-3}}$) from our atomistic values, following Ref.[26]. We remark that the results where the magnetostatic contribution is included are obtained using the modified macrocell approach mentioned in the Methods section. Excellent agreement between the simulated data and the analytic expression for a coherent reversal is found for diameters smaller than 30 nm and 20 nm for calculations with and without magnetostatic interactions, respectively. For larger diameters the data deviate from the above trends and seem to lie in an intermediate regime where there is no available analytic expression. As the diameter is increased further, the data is well fitted by a linear trend as described by the nucleation theory for simulations where $K_{eff} = K_u$. For simulations where the magnetostatic contribution is included, we observe a similar trend. However, a direct comparison with theoretical expressions is not possible due to the complex angle variation of the total magnetostatic field during reversal. A similar analysis has been performed by Chaves-O'Flynn *et al.* [10] by means of a micromagnetic approach at zero temperature and by rescaling the MTJ parameters and size to that of a permalloy disc. The results of Chaves-O'Flynn *et al.* [10] are in good agreement with the analytic expressions for both the macrospin and nucleation regime. We point out that in our opinion using the demagnetisation coefficients to determine K_{eff} for systems with non-uniform magnetisation configurations is not appropriate and leads to an overestimate of the domain wall energy. We attribute the good agreement between the data and the theory in this regime to a combination of the scaling of the magnetic properties of the system and micromagnetic simulations.

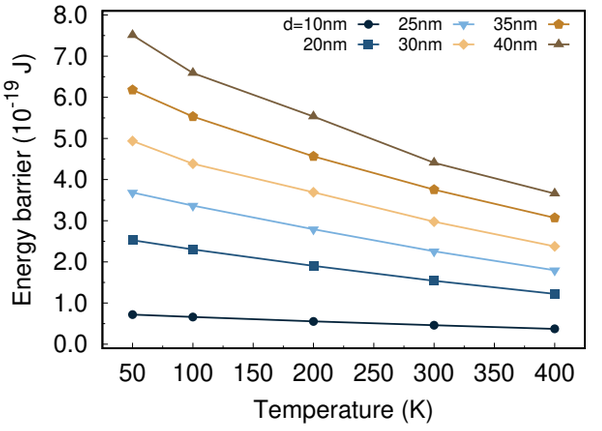

FIG. 3. Plot of the temperature dependence of the energy barrier for different system diameters in the case of simulations with magnetostatic interactions. Lines are a guide to the eye.

Fig. 3 shows the temperature dependence of the energy barrier for different diameters. E_b decreases with increasing temperature and increases with diameter. This increase differs for small and large dots dimensions, in agreement with the analysis of Δ at 300 K indicating that the reversal mechanism depends on the system lateral size: nucleation for large diameters and collinear for dots with diameters smaller than domain wall width. Moreover, the temperature dependence of K_{eff} can be extracted from the calculation of E_b, proving a useful tool to evaluate the properties of the system.

The technological requirement for memory and storage devices is the retention of data, i.e. the magnetic state, for a minimum of ten years. This corresponds to a $\Delta \geq 60$ at room temperature, underlined by the red dashed line in Fig. 2. In our case the smallest element size able to yield the desired thermal stability is around 28 nm when we include the shape anisotropy contribution; hence a smaller system would not satisfy the thermal stability requirements. A solution is to increase the complexity of the stack, as in MTJs with the free

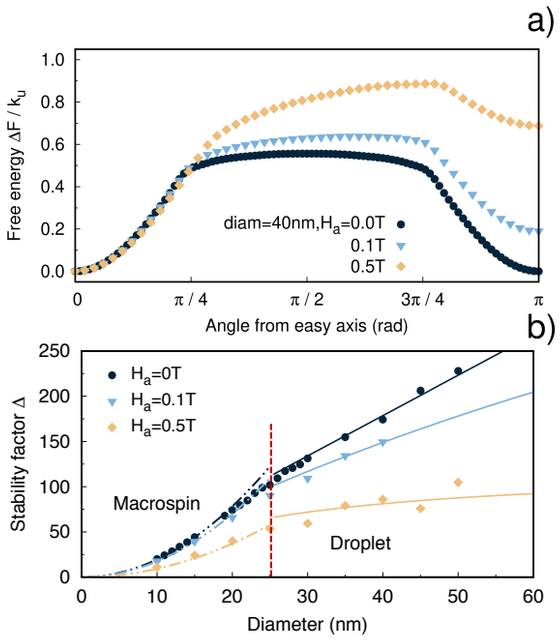

FIG. 4. (a) Angular dependence of the energy barrier normalised by the maximum torque for CoFeB/MgO dots of diameter 40 nm at 300 K for H_a =0.0 T, 0.1 T and 0.5 T applied along the positive z-direction. (b) Thermal stability (Energy barrier/k_BT) as function of diameter for CoFeB/MgO dots at 300 K for an external field as in (a). Points represent the data, solid lines represent the the analytic model describing the droplet theory and dotted lines describe the macrospin model for uniform magnetisation for dimensions smaller than single domain size.

layer composed of a double MgO[3,27] barrier. Such a design helps in reducing the effect of the stray field and is characterised by a larger interfacial anisotropy due to the increased number of CoFeB/MgO interfaces. Another alternative is to fabricate MTJs with an elongated free layer to exploit the shape anisotropy of a rod-like system as an additional source of perpendicular anisotropy, which would allow lateral device dimensions below 10 nm[28–30]. Nevertheless, further studies on both the equilibrium and dynamic properties of such a stack need to be performed to assess the viability of this solution.

B. Effect of an applied field

An applied field acting on the reference layer of a MTJ alters the energy landscape of the layer, and affects the reversal mechanism[22]. For simple MTJ geometries such as a single free layer MTJ[3,7,19], the recording layer is subjected to the stray field coming from the reference layer which can affect the stability of the system[31,32]. We perform simulations at 300 K applying an external field B_a =0.0 T, 0.1 T and 0.5 T along the positive z-direction perpendicular to the dot. Fig. 4(a) depicts the free energy as function of the angle between the total magnetisation and the easy axis for dots of diameter 40 nm at $T = 300$ K for the different B_a. The effect of the external field is to decrease the energy of the minimum corresponding to magnetisation aligned with the external field and to rise the other stable state. As a consequence, the energy barrier between the two stable configurations becomes non-equivalent Similarly to the zero field case, a flattening of the energy barrier at large angle can be observed. However, the application of an external field applied along the stable direction of the magnetisation aids the nucleation and allows the nucleation reversal mechanism at smaller angles. We compare the angular dependence of the energy with that for coherent rotation determined from the extrema of the relevant free energy $K_u \sin^2(\vartheta) - 2B_a \cos(\vartheta)$. For small diameters the coherent energy barrier follows the expected analytic expression for the total energy, as expected for coherent rotation. For larger diameters the system is characterised by a non-uniform reversal mode and the analytic expression cannot reproduce the data.

We compute the energy barrier integrating the torque over the angular dependence and plot the stability factor Δ as a function of particle diameter and applied field at 300 K in Fig. 4(b). For diameters less than 25 nm, close to the single domain size of the system, Δ follows a quadratic behaviour well fit by a macrospin model including the effect of the external field mentioned above, as demonstrated by the dotted lines. Deviations from this behaviour occur as the system size approaches the limiting single domain size and for larger diameters Δ depends linearly on the diameter of the disk, with a slope that decreases for increasing applied fields. In this regime we cannot rely on the macrospin theory, as already seen in the zero field case. In this regime we make a comparison with the droplet theory, Refs.[33–35], which provides an analytic approach to account for the effect of an external field on the energy barrier when the transition between the minimum energy states is non-uniform. We note that the droplet model is essentially a micromagnetic level theory. If magnetostatic fields are neglected, we can write the energy of the droplet as:

$$E^{\text{drop}}(R) = \sigma t \vartheta_d r - 2M_s B_a t \frac{R^2\left[\vartheta - \sin(\vartheta)\right] + r^2\left[\vartheta_d - \sin(\vartheta_d)\right]}{2}, \quad (6)$$

where R, r, ϑ, ϑ_d refer to Fig. 5, σ is the domain wall energy assuming a domain wall at the centre of the system, M_s the saturation magnetisation of the system and B_a is the magnitude of the external applied field. One can easily prove that if $B_a = 0$ T equation 6 reduces to the nucleation model. In the droplet model the energy barrier is determined by the extremum of Eq. 6 subject to the constraint $R\sin(\vartheta/2) = r\sin(\vartheta_D/2)$.

We compare our data for diameters larger than 25 nm with the prediction of the droplet model, represented by the solid lines in Fig. 4(b). The model predicts an asymptotic behaviour of the energy barrier as a function of increasing diameter for a sufficiently strong magnitude of the field. An initial flattening emerges from the results obtained for $B_a = 0.5$ T, however the dependence of the stability factor on large diameters

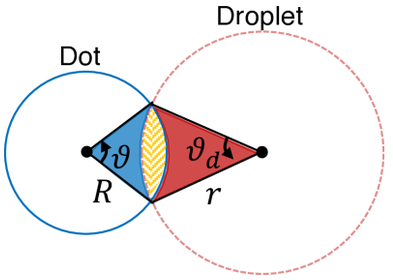

FIG. 5. Sketch showing the parameters used in the calculation of the energy barrier in the droplet model. The reversed magnetised domain is described by the yellow dashed region. The intersection between the blue and red circular sectors within the dot and droplet respectively determines the position and size of the nucleated area. $t\vartheta_{\rm d}r$ is the contact area between the two domains and $\{tR^2[\vartheta-\sin(\vartheta)]+r^2[\vartheta_{\rm d}-\sin(\vartheta_{\rm d})]\}/2$ is the volume of the nucleated domain.

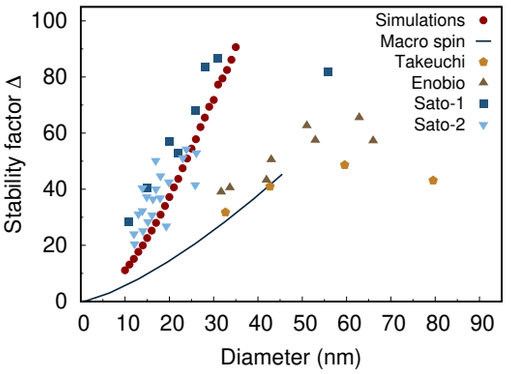

FIG. 6. Comparison between simulated (red dots) stability factor (Energy barrier/$k_{\rm B}T$) as function of diameter for CoFeB/MgO dots at 300 K and experimental results from references[3,5,7]. Sato-1 (blue squares) and Sato-2 (light-blue downwards triangle) refer to series1 and series2 of Ref.[3], respectively. The solid line shows the macrospin model prediction for a system of thickness 1.3 nm.

is required to observe the asymptotic behaviour. In a similar study, Chaves-O'Flynn *et al.*[10] investigate the effect of an external field on the stability of the disc, such as the stray field acting on the free layer of a MTJ coming from the reference layer by means of a zero temperature micromagnetic approach. Chaves-O'Flynn *et al.*[10] predict a saturation of the energy barrier for large diameters, approaching 100 nm or larger, and strong applied fields in agreement with the droplet model. We stress that we did not include the magnetostatic contribution in these simulations to allow a direct comparison with the theoretical droplet model, as it is not clear how to analytically account for this term in the droplet theory formalism. Moreover, we argue that the use of demagnetisation tensors when dealing with non-uniform magnetisation configurations is not appropriate as this is a macroscopic quantity defined in the case of uniform magnetic system.

C. Comparison with experimental results

Finally we compare our simulation results against experiments performed by Sato *et al.*[3], Takeuchi *et al.*[5], Enobio *et al.*[7] in Fig. 6. The simulated data is described by red dots, blue squares and light-blue downwards triangle refer to series1 and series2 of Ref.[3], respectively. Orange diamonds and brown upwards triangles are extracted from the works of Takeuchi *et al.*[5], Enobio *et al.*[7], respectively. The latter two investigate MTJs composed of a single CoFeB/MgO free layer with $K_{\rm eff}\sim 1.9\times10^5\,{\rm Jm}^{-3}$, $M_{\rm s}\sim 1.3\,{\rm T}$ and $A_{\rm s}\sim 30\times10^{-11}\,{\rm Jm}^{-1}$. Sato *et al.*[3] study MTJs with MgO/CoFeB/Ta/CoFeB/MgO recording layer structure characterised by $K_{\rm eff}\sim 9.4\times10^4\,{\rm Jm}^{-3}$, $M_{\rm s}\sim 1\,{\rm T}$ and $A_{\rm s}\sim 20\times10^{-11}\,{\rm Jm}^{-1}$ and as a result are more stable.

We can see that our simulations agree with the data from Ref.[3] up to diameters of 35 nm, where for small diameters data and simulations agree with a microspin model, whereas for large dimensions follow a linear trend characteristic of nucleation. On the other hand, the stability factor results from our simulations are much larger than those reported by Takeuchi and collaborators in Ref.[5] and Enobio and collaborators in Ref.[7]. Takeuchi *et al.*[5] and Enobio *et al.*[7] studied MTJs with lower perpendicular anisotropy than in our simulations, which can explain our larger energy barriers. We parametrise the macrospin model for $E_{\rm b}$ using our atomistic parameters and we estimate the size dependence of Δ for a dot of thickness 1.3 nm within the expected uniform reversal region, shown by the solid line in Fig. 6. Our prediction seems to agree with the experimental data in Ref.[5,7] for diameters smaller than the critical domain size, estimated around 45 nm. However, we need calculations to prove the agreement, calculations that become particularly intensive at large dimensions and can become the object of future work.

The incidental agreement between experiments performed on MTJs with a double MgO layer[3] and our simulations is unexpected since we simulate a single CoFeB/MgO free layer and the two structures are not comparable in properties. We can speculate that the small thickness used in our simulations, 1 nm, yields a $K_{\rm eff}$ similar to the double stack studied in the experiments. However, to assess more realistically an agreement we would need to perform energy barrier calculations on an analogous system. We also point out that in our simulations we do not account for structural defects and fabrication damage, something that occurs in real devices.

Finally, we can observe that Sato *et al.*[3] and Takeuchi *et al.*[5] obtain a value of Δ which suggests a constant $E_{\rm b}$ for large diameters, rather far from the single domain size of their systems, which they associate to nucleation mechanisms. While we agree on the nature of the reversal mechanism for such dimensions, we believe that Δ should still show a dependence on the diameter of the dots, even for large dimensions. In both these works $E_{\rm b}$ is obtained by measuring the switching probability as a function of the magnitude of the applied magnetic field and such fields might affect $E_{\rm b}$. Another possible reason for the constant trend could be the presence of fringe

fields due to the reference layer of the MTJ[31,32] that could reduce E_b, as also discussed in the analysis of the effect of an external field. We remark that the thermal stability is one the main parameters for MRAM technology since it affects both the data retention of a device and the writing performances via the threshold current. As a consequence, understanding the size, temperature and field dependence of the energy barrier is fundamental for future improvements of this technology.

Overall our results demonstrate the ability of an atomistic spin model to calculate the energy barrier for technologically relevant sizes of realistic MTJs at pertinent temperatures yielding values close to experiments, even in the nucleation regime where the magnetostatic contribution needs to be accurately accounted for.

IV. CONCLUSIONS

The energy barrier is the key parameter in the thermal stability of magnetic tunnel junctions, the main component of MRAM devices, and needs to be characterised. To deal with the devices at the nanoscale we have used an atomistic spin model to investigate the size, temperature and field dependence of the energy barrier in ultra thin CoFeB/MgO discs comprising the free layers of magnetic tunnel junctions. We have found that a transition from coherent to domain wall mediated reversal occurs around the critical domain size at about 30 nm. These two regimes are not separated by a sharp transition and the intermediate region is not captured by analytic descriptions. Therefore it is important to have approaches that provide understanding and are able to accurately characterise the thermal stability at dimensions that are of significant technological interest. Atomistic models can simulate excitations at all lengthscales and should be considered benchmark calculations. It is interesting that in the limit of large dot sizes our calculations give energy barriers similar to the droplet (continuum) model, this is true in the case of an external applied field as well. This suggests that for simple systems without complex magnetic properties, such as for instance Dzyaloshinskii-Moriya interactions, micromagnetic models with atomistic parametrisation are applicable without introducing the anisotropy phenomenologically. To conclude, we have shown that the atomistic spin model parametrised using realistic values can extract and characterise the energy barrier in systems that are at the state of the art and can provide guidance to experiments identifying suitable materials and MTJ stacks with the desired thermal stability. We remark that ours is an initial investigation and that in order to achieve a complete characterisation of the various parameters contributions to the energy barrier would require additional studies.

ACKNOWLEDGEMENTS

The authors gratefully acknowledge funding from the Samsung SGMI programme.

AUTHOR CONTRIBUTIONS

AM performed the atomistic simulations, analysed the results and drafted the paper. AM, RFLE and RWC conceived and designed the study. All authors contributed to the writing of the paper.

AIP PUBLISHING DATA SHARING POLICY

The data that support the findings of this study are available from the corresponding author upon reasonable request.

[1] H. Sato, M. Yamanouchi, K. Miura, S. Ikeda, H. D. Gan, K. Mizunuma, R. Koizumi, F. Matsukura, and H. Ohno, "Junction size effect on switching current and thermal stability in CoFeB/MgO perpendicular magnetic tunnel junctions," Applied Physics Letters **99**, 042501 (2011), 10.1063/1.3617429.
[2] H. Sato, M. Yamanouchi, K. Miura, S. Ikeda, R. Koizumi, F. Matsukura, and H. Ohno, "CoFeB Thickness Dependence of Thermal Stability Factor in CoFeB/MgO Perpendicular Magnetic Tunnel Junctions," Magnetics Letters, IEEE **3**, 3000204–3000204 (2012).
[3] H. Sato, E. C. I. Enobio, M. Yamanouchi, S. Ikeda, S. Fukami, S. Kanai, F. Matsukura, and H. Ohno, "Properties of magnetic tunnel junctions with a MgO CoFeB Ta CoFeB MgO recording structure down to junction diameter of 11nm," Applied Physics Letters **105**, 062403 (2014), 10.1063/1.4892924.
[4] J. Z. Sun, S. L. Brown, W. Chen, E. A. Delenia, M. C. Gaidis, J. Harms, G. Hu, X. Jiang, R. Kilaru, W. Kula, G. Lauer, L. Q. Liu, S. Murthy, J. Nowak, E. J. O'Sullivan, S. S. P. Parkin, R. P. Robertazzi, P. M. Rice, G. Sandhu, T. Topuria, and D. C. Worledge, "Spin-torque switching efficiency in CoFeB-MgO based tunnel junctions," Physical Review B **88**, 104426 (2013).
[5] Y. Takeuchi, H. Sato, S. Fukami, F. Matsukura, and H. Ohno, "Temperature dependence of energy barrier in CoFeB-MgO magnetic tunnel junctions with perpendicular easy axis," Applied Physics Letters **107**, 152405 (2015), 10.1063/1.4933256.
[6] M. Gajek, J. J. Nowak, J. Z. Sun, P. L. Trouilloud, E. J. O'Sullivan, D. W. Abraham, M. C. Gaidis, G. Hu, S. Brown, Y. Zhu, R. P. Robertazzi, W. J. Gallagher, and D. C. Worledge, "Spin torque switching of 20 nm magnetic tunnel junctions with perpendicular anisotropy," Applied Physics Letters **100**, 132408 (2012).
[7] E. C. I. Enobio, M. Bersweiler, H. Sato, S. Fukami, and H. Ohno, "Evaluation of energy barrier of CoFeB/MgO magnetic tunnel junctions with perpendicular easy axis using retention time measurement," Japanese Journal of Applied Physics **57**, 04FN08 (2018).
[8] K. Munira and P. B. Visscher, "Calculation of energy-barrier lowering by incoherent switching in spin-transfer torque magnetoresistive random-access memory," Journal of Applied Physics **117**, 17B710 (2015).
[9] G. D. Chaves-O'Flynn, E. Vanden-Eijnden, D. L. Stein, and A. D. Kent, "Energy barriers to magnetization reversal in perpendicularly magnetized thin film nanomagnets," Journal of Applied Physics **113**, 023912 (2013).
[10] G. D. Chaves-O'Flynn, G. Wolf, J. Z. Sun, and A. D. Kent, "Thermal Stability of Magnetic States in Circular Thin-Film Nanomagnets with Large Perpendicular Magnetic Anisotropy," Phys. Rev. Applied **4**, 024010 (2015).
[11] R. Cuadrado, L. Oroszlány, A. Deák, T. A. Ostler, A. Meo, R. V. Chepulskii, D. Apalkov, R. F. L. Evans, L. Szunyogh, and R. W. Chantrell, "Site-Resolved Contributions to the Magnetic-Anisotropy Energy and Complex Spin Structure of Fe/MgO Sandwiches," Phys. Rev. Applied **9**, 054048 (2018).
[12] H. X. Yang, M. Chshiev, B. Dieny, J. H. Lee, A. Manchon, and K. H. Shin, "First-principles investigation of the very large perpendicular magnetic anisotropy at Fe/MgO and Co/MgO interfaces," Phys. Rev. B **84**, 054401 (2011).
[13] I. Turek, S. Blugel, G. Bihlmayer, and P. Weinberger, "Exchange Interactions at Surfaces of Fe, Co, and Gd," Czechoslovak Journal of Physics **53**, 81–88 (2003).
[14] "Computer code VAMPIRE," (2013).

[15]G. J. Bowden, G. B. G. Stenning, and G. van der Laan, "Inter and intra macro-cell model for point dipole–dipole energy calculations," Journal of Physics: Condensed Matter **28**, 066001 (2016).
[16]P. Asselin, R. F. L. Evans, J. Barker, R. W. Chantrell, R. Yanes, O. Chubykalo-Fesenko, D. Hinzke, and U. Nowak, "Constrained Monte Carlo method and calculation of the temperature dependence of magnetic anisotropy," Phys. Rev. B **82**, 054415 (2010).
[17]J. D. Alzate-Cardona, D. Sabogal-Suárez, R. F. L. Evans, and E. Restrepo-Parra, "Optimal phase space sampling for Monte Carlo simulations of Heisenberg spin systems," Journal of Physics: Condensed Matter **31**, 095802 (2019).
[18]H. Sato, P. Chureemart, F. Matsukura, R. W. Chantrell, H. Ohno, and R. F. L. Evans, "Temperature-dependent properties of CoFeB/MgO thin films: Experiments versus simulations," Physical Review B **98**, 214428 (2018).
[19]S. Ikeda, K. Miura, H. Yamamoto, K. Mizunuma, H. D. Gan, M. Endo, S. Kanai, J. Hayakawa, F. Matsukura, and H. Ohno, "A perpendicular-anisotropy CoFeB–MgO magnetic tunnel junction," Nature Materials (2010).
[20]R. F. L. Evans, W. J. Fan, P. Chureemart, T. A. Ostler, M. O. A. Ellis, and R. W. Chantrell, "Atomistic spin model simulations of magnetic nanomaterials," Journal of Physics: Condensed Matter **26**, 103202 (2014).
[21]D. A. Garanin, "Self-consistent Gaussian approximation for classical spin systems: Thermodynamics," Phys. Rev. B **53**, 11593–11605 (1996).
[22]A. Meo, P. Chureemart, S. Wang, R. Chepulskyy, D. Apalkov, R. W. Chantrell, and R. F. L. Evans, "Thermally nucleated magnetic reversal in CoFeB/MgO nanodots," Scientific Reports **7**, 16729 (2017).
[23]T. Devolder, P. Ducrot, J. Adam, I. Barisic, N. Vernier, J.-v. Kim, B. Ockert, and D. Ravelosona, "Damping of Co x Fe 80 2x B 20 ultrathin films with perpendicular magnetic anisotropy," Applied Physics Letters **022407**, 4–7 (2013).
[24]S. Sampan-a pai, J. Chureemart, R. W. Chantrell, R. Chepulskyy, S. Wang, D. Apalkov, R. F. L. Evans, and P. Chureemart, "Temperature and Thickness Dependence of Statistical Fluctuations of the Gilbert Damping in CoFeB/MgO bilayers," Physical Review Applied **11**, 044001 (2019).
[25]R. Skomski, *Simple Models of Magnetism* (Oxford university press, 2008).
[26]R. Moreno, R. F. L. Evans, S. Khmelevskyi, M. C. Muñoz, R. W. Chantrell, and O. Chubykalo-Fesenko, "Temperature-dependent exchange stiffness and domain wall width in Co," Physical Review B **94**, 104433 (2016).
[27]E. Liu, J. Swerts, Y. C. Y. Wu, A. Vaysset, S. Couet, S. Mertens, S. Rao, W. Kim, S. Van Elshocht, J. De Boeck, and G. G. S. Kar, "Top-Pinned STT-MRAM Devices With High Thermal Stability Hybrid Free Layers for High-Density Memory Applications," IEEE Transactions on Magnetics , 1–5 (2018).
[28]N. Perrissin, S. Lequeux, N. Strelkov, A. Chavent, L. Vila, L. D. Buda-Prejbeanu, S. Auffret, R. C. Sousa, I. L. Prejbeanu, and B. Dieny, "A highly thermally stable sub-20 nm magnetic random-access memory based on perpendicular shape anisotropy," Nanoscale **10**, 12187–12195 (2018).
[29]K. Watanabe, B. Jinnai, S. Fukami, H. Sato, and H. Ohno, "Shape anisotropy revisited in single-digit nanometer magnetic tunnel junctions," Nature Communications **9**, 663 (2018).
[30]N. Perrissin, G. Gregoire, S. Lequeux, L. Tillie, N. Strelkov, S. Auffret, L. D. Buda-Prejbeanu, R. C. Sousa, L. Vila, B. Dieny, and I. L. Prejbeanu, "Perpendicular shape anisotropy spin transfer torque magnetic random-access memory: towards sub-10 nm devices," Journal of Physics D: Applied Physics **52**, 234001 (2019).
[31]M. Bapna, S. K. Piotrowski, S. D. Oberdick, M. Li, C.-L. Chien, and S. A. Majetich, "Magnetostatic effects on switching in small magnetic tunnel junctions," Applied Physics Letters **108**, 022406 (2016).
[32]S. Jenkins, A. Meo, L. E. Elliott, S. K. Piotrowski, M. Bapna, R. W. Chantrell, S. A. Majetich, and R. F. L. Evans, "Magnetic stray fields in nanoscale magnetic tunnel junctions," Journal of Physics D: Applied Physics (2019).
[33]D. Hinzke and U. Nowak, "Magnetization switching in a Heisenberg model for small ferromagnetic particles," Physical Review B **58**, 265–272 (1998).
[34]D. Hinzke and U. Nowak, "Monte Carlo simulation of magnetization switching in a Heisenberg model for small ferromagnetic particles," Computer Physics Communications **121-122**, 334–337 (1999).
[35]U. Nowak and D. Hinzke, "Magnetization switching in small ferromagnetic particles: Nucleation and coherent rotation," Journal of Applied Physics **85**, 4337–4339 (1999).
[36]Hubert Alex and R. Schäfer, *Magnetic Domains: The Analysis of Magnetic Microestructures*, Vol. 40 (1998) p. 109.
[37]H. Callen and E. Callen, "The present status of the temperature dependence of magnetocrystalline anisotropy, and the power law," Journal of Physics and Chemistry of Solids **27**, 1271–1285 (1966).
[38]J.-H. Kim, J.-B. Lee, G.-G. An, S.-M. Yang, W.-S. Chung, H.-S. Park, and J.-P. Hong, "Ultrathin W space layer-enabled thermal stability enhancement in a perpendicular MgO/CoFeB/W/CoFeB/MgO recording frame," Sci. Rep. **5**, 16903 (2015).
[39]a. V. Khvalkovskiy, D. Apalkov, S. Watts, R. Chepulskii, R. S. Beach, a. Ong, X. Tang, a. Driskill-Smith, W. H. Butler, P. B. Visscher, D. Lottis, E. Chen, V. Nikitin, and M. Krounbi, "Basic principles of STT-MRAM cell operation in memory arrays," J. Phys. D. Appl. Phys. **46**, 074001 (2013).
[40]P. H. Jang, K. Song, S. J. Lee, S. W. Lee, and K. J. Lee, "Detrimental effect of interfacial Dzyaloshinskii-Moriya interaction on perpendicular spin-transfer-torque magnetic random access memory," Appl. Phys. Lett. **107** (2015), 10.1063/1.4936089.
[41]J. Sampaio, A. V. Khvalkovskiy, M. Kuteifan, M. Cubukcu, D. Apalkov, V. Lomakin, V. Cros, and N. Reyren, "Disruptive effect of Dzyaloshinskii-Moriya interaction on the magnetic memory cell performance," Applied Physics Letters **108**, 112403 (2016).
[42]M. Ležaić, P. Mavropoulos, and S. Blügel, "First-principles prediction of high Curie temperature for ferromagnetic bcc-Co and bcc-FeCo alloys and its relevance to tunneling magnetoresistance," Applied Physics Letters **90**, 0–3 (2007).

AIP Publishing

Journal of Applied Physics

PLEASE CITE THIS ARTICLE AS DOI: 10.1063/5.0018909

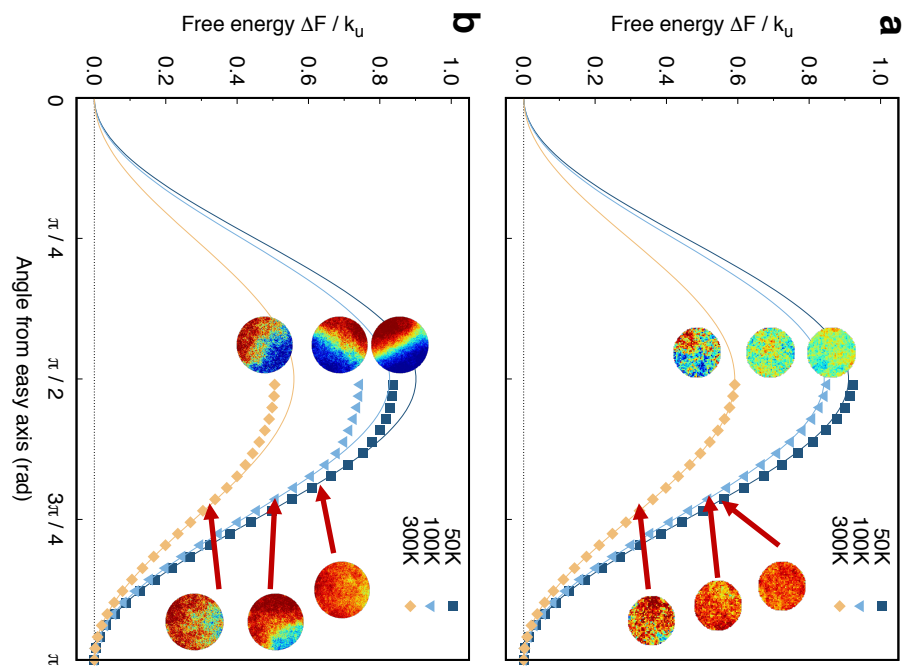

AIP Publishing

Journal of Applied Physics

PLEASE CITE THIS ARTICLE AS DOI: 10.1063/5.0018909

AIP Publishing

Journal of Applied Physics

PLEASE CITE THIS ARTICLE AS DOI: 10.1063/5.0018909

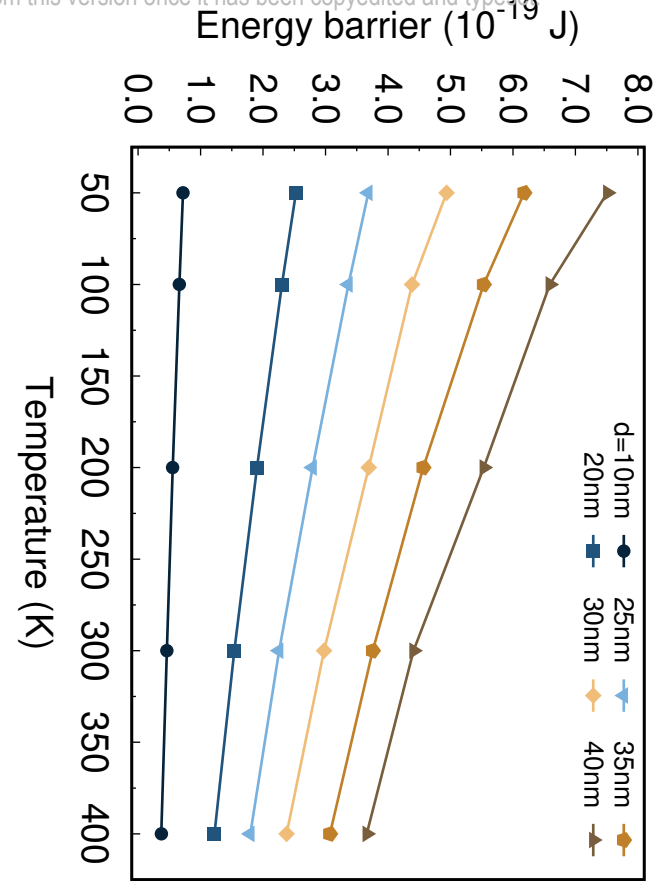

AIP Publishing

Journal of Applied Physics

PLEASE CITE THIS ARTICLE AS DOI: 10.1063/5.0018909

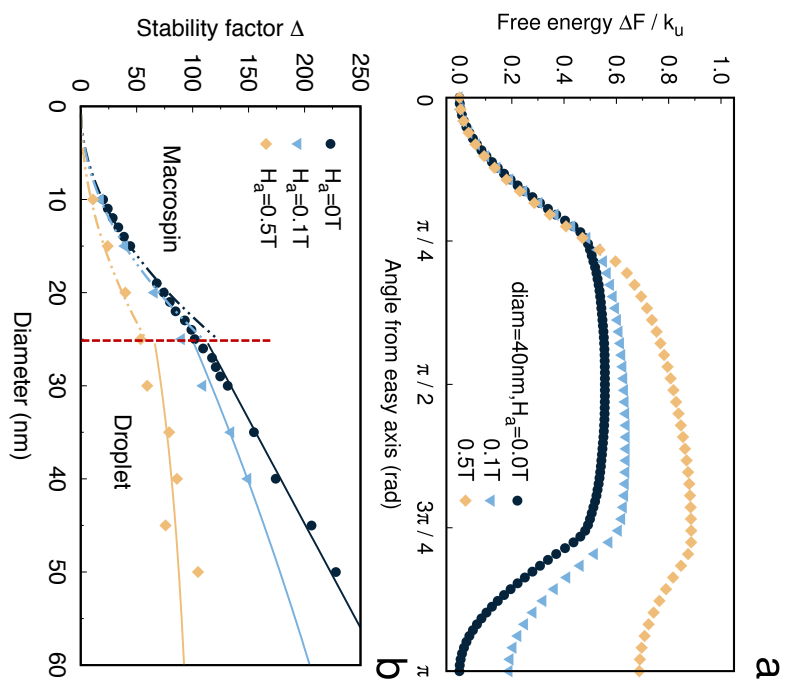

AIP Publishing

Journal of Applied Physics

ACCEPTED MANUSCRIPT

PLEASE CITE THIS ARTICLE AS DOI: 10.1063/5.0018909

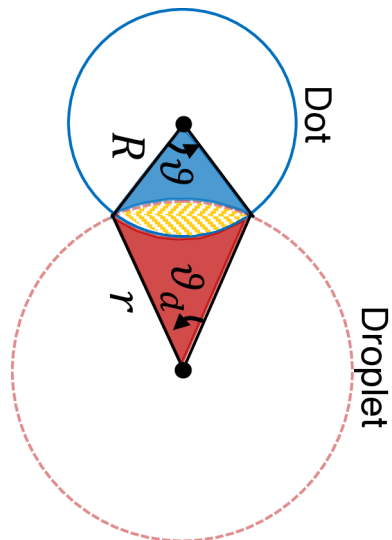

AIP Publishing

Journal of Applied Physics

PLEASE CITE THIS ARTICLE AS DOI: 10.1063/5.0018909